A role for JAK2 in mediating cell surface GHR-PRLR interaction

Chen Chen[1,2], Jing Jiang[2], Tejeshwar C. Rao[3], Tatiana T. Marquez Lago[1], Stuart J. Frank[*2], André Leier[*1]

[1]Department of Genetics, University of Alabama at Birmingham, Birmingham, USA
[2]Division of Endocrinology, Diabetes, and Metabolism, Department of Medicine, University of Alabama at Birmingham, Birmingham, USA
[3]Department of Cell, Developmental, and Integrative Biology, University of Alabama at Birmingham, Birmingham, USA

[*]Co-corresponding authors

Abstract

Growth hormone (GH) receptor (GHR) and prolactin (PRL) receptor (PRLR) are transmembrane class I cytokine receptors that co-exist in various normal and cancerous cells. Both receptors respond to their associated ligands predominantly by activating the Janus Kinase 2 (JAK2)-signal transducer and activator of transcription (STAT) signaling pathways, and both are also known to initiate receptor-specific JAK2-independent signaling. Together with their cognate ligands, these receptors have been associated with pro-tumorigenic effects in various cancers, including breast cancer (BC). Human GH is known to bind GHR and PRLR, while PRL can only bind PRLR. A growing body of work suggests that GHR and PRLR can form heteromers in BC cells, modulating GH signal transduction. However, the dynamics of PRLR and GHR on the plasma membrane and how these could affect their respective signaling still need to be understood.

To this end, we set out to unravel the spatiotemporal dynamics of GHR and PRLR on the surface of human T47D breast cancer cells and γ2A-JAK2 cells. We applied direct stochastic optical reconstruction microscopy (dSTORM) and quantified the colocalization and availability of both receptors on the plasma membrane at the nanometer scale at different time points following treatment with GH and PRL. In cells co-expressing GHR and PRLR, we surprisingly observed that not only GH but also PRL treatment induces a significant loss of surface GHR. In cells lacking PRLR or expressing a mutant PRLR deficient in JAK2 binding, we observed that GH induces downregulation of membrane-bound GHR, but PRL no longer induces loss of surface GHR. Colocalizations of GHR and PRLR were confirmed by proximity ligation (PL) assay.

Our results suggest that PRLR-GHR interaction, direct or indirect, is indispensable for PRL- but not GH-induced loss of surface GHR and for both GH-induced and PRL-induced increase of surface PRLR, with potential consequences for downstream signaling. Furthermore, our results suggest that JAK2 binding via the receptor intracellular domain's Box1 element is crucial for the observed regulation of one class I cytokine receptor's cell surface availability via ligand-induced activation of another class I cytokine receptor. Our findings shed new light on the reciprocal and collective role that PRLR and GHR play in regulating cell signaling.

Keywords: growth hormone receptor, prolactin receptor, Box1, JAK2, super-resolution microscopy, direct stochastic optical reconstruction microscopy (dSTORM)

Introduction

Growth hormone (GH) and prolactin (PRL) are hormones emanating mainly from the anterior pituitary. The primary function of GH is regulating anabolism and metabolism [1, 2], while PRL has important roles in breast development and lactation [3]. There is mounting evidence pointing at both hormones and their receptors playing roles in various types of cancer [4-11], including breast cancer (BC) [12-17], where GHR is frequently present and PRLR is often found overexpressed [18-25]. While they have been mostly associated with pro-tumorigenic effects, PRL has also been reported to show anti-tumor effects and, like PRLR, has been associated with good prognosis in certain BC subtypes [26-29]. However, a humanized neutralizing monoclonal antibody directed against the extracellular domain of PRLR showed no anti-tumor effect when administered in patients with PRLR-positive metastatic BC [30]. This suggests that PRLRs' pro-tumorigenic function may not be as relevant as previously thought or depends on other circumstances such as the presence or absence of other hormone receptors, with which they may interact.

Both GH receptor (GHR) and PRL receptor (PRLR) are structurally similar transmembrane glycoproteins and belong to the class I cytokine receptor superfamily [31, 32]. GH can bind and introduce a conformational change to both GHR and PRLR, allowing receptor activation and downstream signaling [33-37], but, unlike GH, PRL can only bind to PRLR [36, 38-40]. Both GHR and PRLR lack intrinsic kinase activity. However, as is characteristic of their superfamily members, both receptors contain a proline-rich Box1 motif in the membrane-proximal region of their intracellular domains (ICDs). Following ligand binding, downstream signal transduction involves predominantly activating the associated cytoplasmic tyrosine kinase, Janus kinase 2 (JAK2), bound to the receptors' Box1 elements. This is followed by phosphorylation of the signal transducer and activator of transcription 5 (STAT5) [41, 42], although other receptor-specific JAK2-independent signal transduction pathways may also be activated.

Increasing evidence indicates that GHR and PRLR interact. Two decades ago, it was shown that ovine GHR (oGHR) and PRLR (oPRLR) can tightly associate with each other following stimulation with placental lactogen [43]. These studies utilized chimeric receptors consisting of the extracellular domain (ECD) of human granulocyte and macrophage colony-stimulating factor (hGM-CSF) receptor (hGM-CSFR) along with a part of either oGHR ICD or oPRLR ICD. After hGM-CSF treatment of cells co-expressing oGHR chimera and oPRLR chimera, JAK2 was effectively activated, and protein-protein interaction of both chimeric receptors was detected via co-immunoprecipitation [43, 44]. Additionally, our previous work revealed a specific ligand-independent human GHR (hGHR) - human PRLR (hPRLR) association in human T47D breast cancer cells, which endogenously express both receptors [45]. Further, the use of split luciferase complementation assays has suggested that hGHR homodimers and hPRLR homodimers form hGHR/hPRLR multimers [46] and extracellular subdomain 2 of the hGHR or hPRLR determines the dimerization partner [47]. Although biochemical studies and luciferase complementation assays strongly support the notion that an interplay between hGHR and hPRLR exists, the observed outcomes are ascribed to total receptors within cells, irrespective of subcellular localization.

In the present study, we directly visualized the cell surface interaction of hGHR and hPRLR and how it changes upon ligand treatment. Specifically, we used direct stochastic optical reconstruction microscopy (dSTORM) [48] to visualize single receptor clusters of hGHR and hPRLR on cell surfaces. In dSTORM, a super-resolution microscopy technique, individual fluorophores cycle through reversible transitions between a dark and a fluorescent state [49]. Thus, a fluorophore emits photons multiple times before

permanently being photobleached. These blinking events and their localizations are recorded and, although the exact number of proteins in clusters is difficult to determine, the number of localizations is strongly correlated with the number of receptors [50, 51]. Thus, the dSTORM approach can deliver high-resolution images to reveal the localization or arrangement of individual membrane receptor systems providing valuable insight into their interactions with other proteins at the cell surface. Given that receptors are highly trafficked to and from the cell surface and to avoid signal detection from cytosolic receptors, we used monoclonal antibodies to distinctly label the extracellular S2 domain of GHR and PRLR on non-permeabilized cells. Descriptive spatial analysis using Ripley's K- and L-function [52] indicates that both hGHR and hPRLR are organized in nanometer-scale clusters on the T47D cell surface. To further gain quantitative information about GHR and PRLR nanoclusters, we applied DBSCAN (density-based spatial clustering of applications with noise) [53]. Subsequently, individual cluster contours were delineated, individual clusters were assigned a cluster ID, and receptor abundance was analyzed separately for each cluster and receptor. By doing so, we detected and calculated homomeric and heteromeric hGHR and hPRLR clusters on cell surfaces. Colocalizations of GHR and PRLR were also confirmed by proximity ligation (PL) assay. Lastly, we explored which receptor domains determine the interaction of hGHR and hPRLR by creating different truncated or modified hPRLR variants. Our findings indicate that the intracellular Box1 region is an essential determinant of hGHR and hPRLR association, suggesting JAK2 may play an important role in the observed ligand-induced and PRLR-mediated downregulation of GHR – which could also elicit or add to PRLR's observed anti-tumor effect.

Results

Ligands induce an increase in PRLR localizations and a decrease in GHR localizations at the surface of T47D cells

To investigate the dynamic spatial distribution of endogenous hGHR and hPRLR on the surface of breast cancer cells, we used dSTORM under the total internal reflection fluorescence (TIRF) illumination mode [54]. The dSTORM images show that hGHR and hPRLR form nanometer-scale clusters and are broadly distributed on the surface of T47D cells (Fig. 1). To assess the ligands' effects on the spatial distribution of hGHR and hPRLR on the cell surface, we conducted time-course experiments using T47D cells with human GH or human PRL (500 ng/ml each). Such stimulation is known to induce rapid and substantial STAT5 phosphorylation [45]. We first analyzed the cell surface localization density (number of localizations per μm^2) of hGHR or hPRLR in both resting and ligand-stimulated conditions. The abundance of surface-hPRLR was rapidly increased, reaching its maximum after 3 min of GH or PRL treatment with a ~5.6-fold and ~4.5-fold increase compared to the basal value, respectively (Fig. 2A and 2B). This increase was followed by a rapid decline: after GH treatment for 5 min, the localization density dropped from 200.6 ± 14.7 per μm^2 to 57.2 ± 3.6 per μm^2; after PRL treatment for 5 min, the density fell from 159.4 ± 16.2 per μm^2 to 94.8 ± 16.0 per μm^2. In contrast to hPRLR, the density of hGHR significantly decreased from 43.3 ± 5.5 per μm^2 basally to 25.8 ± 2.7 per μm^2 after 3min of GH stimulation. After 5 min and 10 min of GH stimulation, the density of hGHR remained relatively low at 26.6 ± 2.3 per μm^2 and 19.3 ± 1.5 per μm^2, respectively (Fig. 2C). Surprisingly, PRL, which does not bind to hGHR, also induced a loss of surface hGHR on T47D cells. After 1 min of PRL treatment, only 36% of hGHR remained on the cell surface compared to the basal state, and hGHR density remained low for at least 10 min (Fig. 2D). A schematic illustration of GH- and PRL-induced hGHR and hPRLR density changes is shown in Fig. 2E. We previously observed that hGHR and

121 hPRLR specifically co-immunoprecipitate in the absence of added ligands in T47D cells [45]; thus, we
122 postulate that the propensity of hGHR and hPRLR to physically interact underlies our observed loss of
123 hGHR in response to PRL stimulation.

124

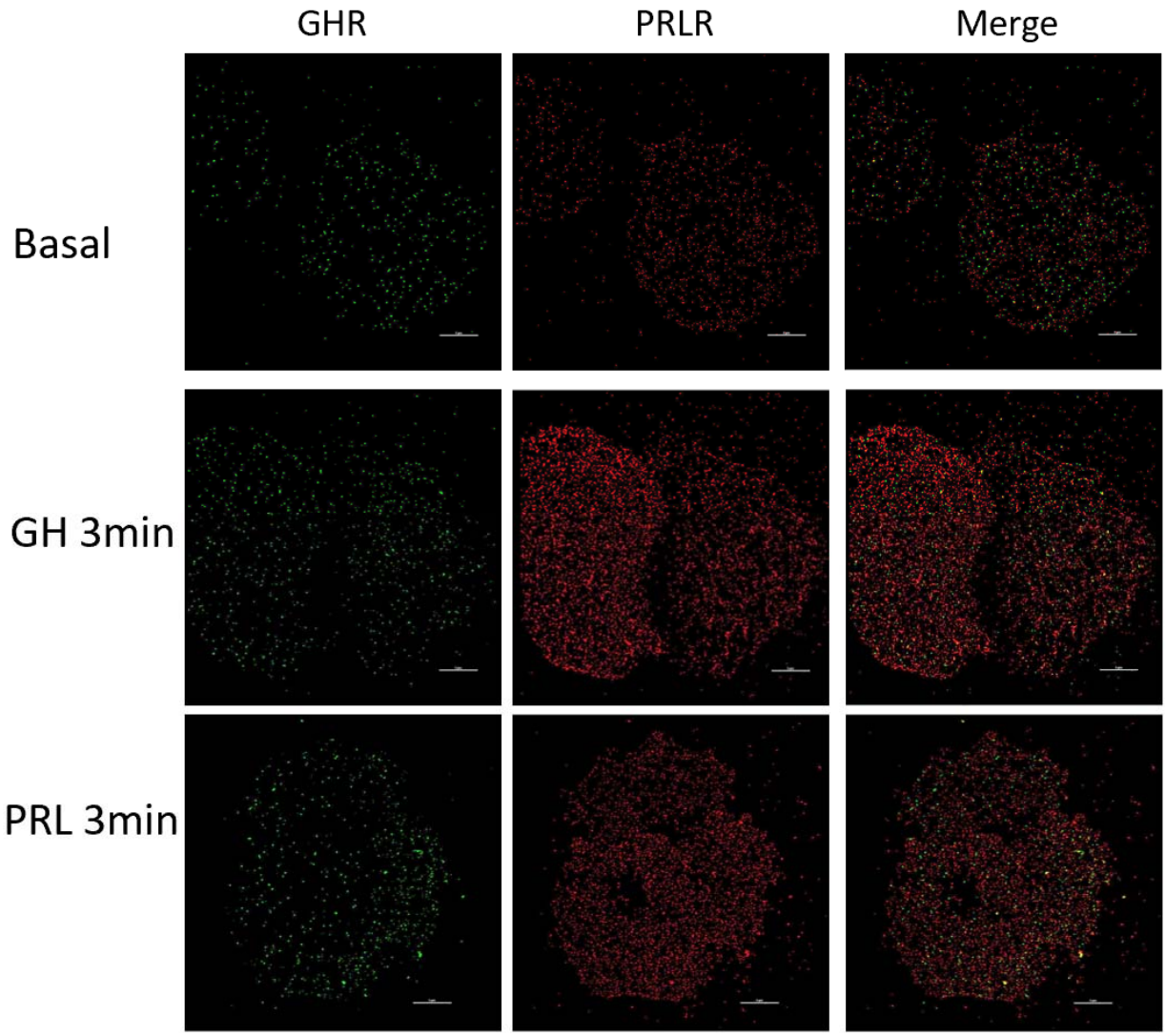

125

126 **Fig. 1.** Ligand-induced increase of PRLR localizations and decrease of GHR localizations at the surface of
127 T47D cells. A representative set of reconstructed dSTORM images. GHR is labeled with Alexa 568-
128 conjugated antibody (green, channel 1), and PRLR is labeled with Alexa 647-conjugated antibody (red,
129 channel 2). The last column of images shows the merging of these two channels. T47D cells were either
130 left untreated (upper row), exposed to 500ng/mL GH for 3 min (middle row), or exposed to 500ng/mL PRL
131 for 3 min (lower row). Brightness was increased by 40% and Contrast was reduced by 40% to increase
132 visibility. Scale bars 5µm.

133

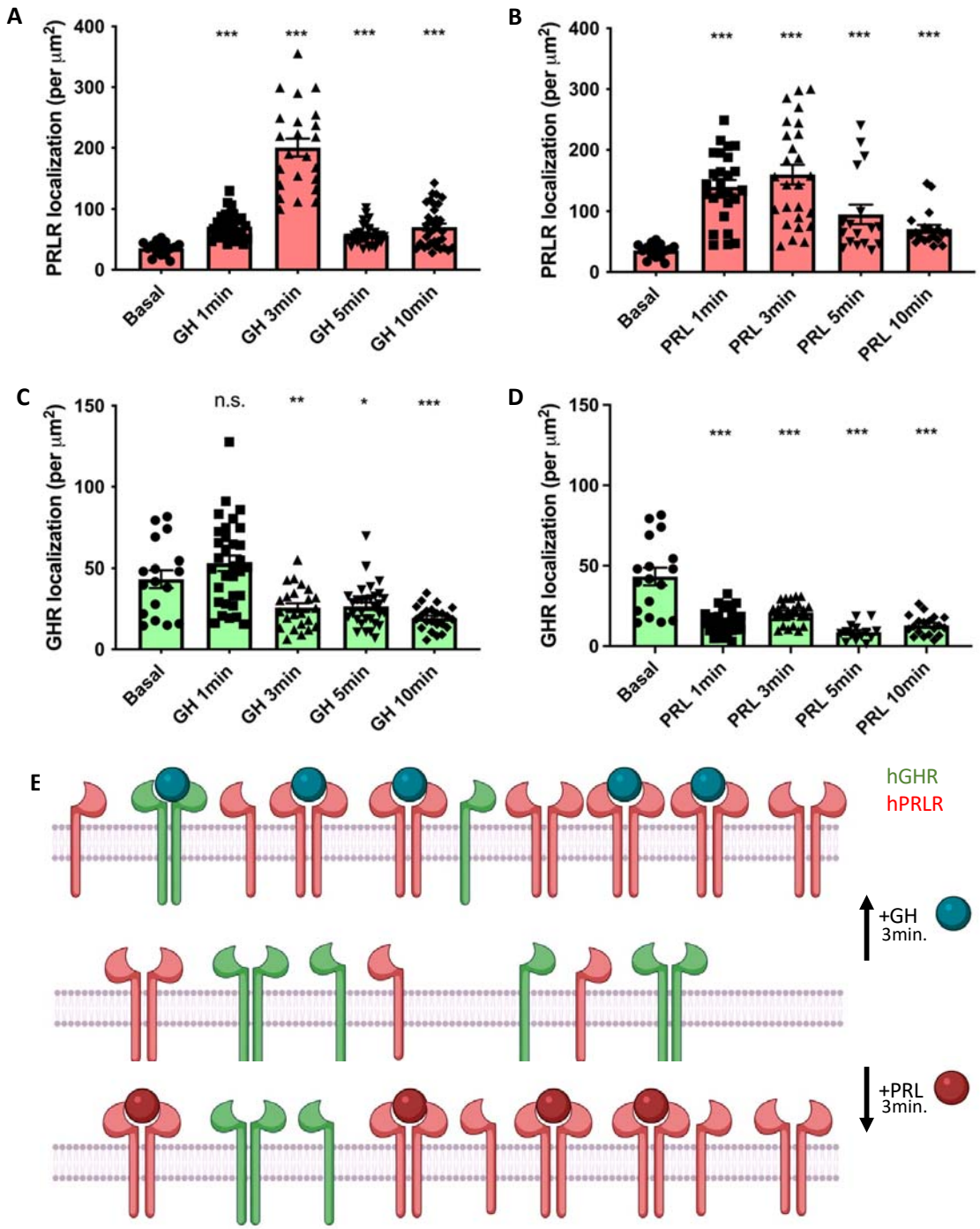

Fig. 2. (A, B) Quantification of GH-induced (500 ng/ml) (A) and PRL-induced (500 ng/ml) (B) changes of PRLR localizations on the cell surface. **(C, D)** Quantification of GH-induced (C) and PRL-induced (D) changes of GHR localizations on the cell surface. Each data point represents the density of receptors in a 6.25 µm X 6.25 µm area. Data are collected from at least 6 cells from each group and displayed as mean ± SE. * (P<0.05), ** (P<0.01), and *** (P<0.001) indicate the statistical significance in comparison with Basal and are calculated by two-tailed t-tests assuming unequal variances. **(E)** Model depicting hPRLR and hGHR densities and activation schemes in T47D cells.

GH or PRL stimulation induces a redistribution of hGHR and hPRLR clusters

We analyzed the dSTORM images using the DBSCAN algorithm to identify different clusters and determine the number of receptor localizations within a cluster (termed 'cluster size') (Fig. 3A). We then performed a localization distribution analysis and plotted a histogram of the relative frequency of localizations (termed 'distribution plot' in this study). Representative dSTORM images of hGHR as well as associated distribution plots are shown in Fig. 3B.

To gain a better understanding of the changes in GHR-PRLR colocalizations, we obtained and analyzed the corresponding bivariate cluster size distributions. Their median values are summarized in Fig. 3C and 3D. As can be seen, hGHR responds quickly and transiently to GH stimulation by forming larger clusters. After GH treatment for 1 min, the median number of hGHR blinking events in a cluster reaches its peak and amounts to 85.6 ± 20.9 localizations in comparison with 33.3 ± 1.7 localizations per cluster in the basal state (P value = 0.0035). After 5 min, this number is reduced approximately to its pre-stimulation value (29.1 ± 2.2) but appears to continue to fluctuate for at least another 25 minutes (Fig. 3C). In turn, hPRLR responds to GH in a less prominent manner: The median number of hPRLR blinking events in a cluster in the basal state is 16.5 ± 0.7. After 3 min of GH stimulation, the median of PRLR cluster size reaches its maximum, which is 22.5 ± 3.9 (P value = 0.1496), and afterward declines to its basal level (Fig. 3C).

Like the response to GH, hGHR reacts also quickly to PRL treatment. The median number of hGHR blinking events in a cluster culminates at 1 min of PRL treatment with 45.8 ± 5.0 (compared with basal level, P value = 0.0098). In distinction, hPRLR response to PRL is slower. The median number of hPRLR blinking events in a cluster reaches its peak at 5 min of PRL treatment with a median number of 23.3 ± 2.8 (compared with basal level, P value = 0.0233), and after 10 min the median is only slightly less than that maximum (Fig. 3D). Together, these results indicate that upon ligand stimulation hGHR cluster sizes increase transiently and significantly, while changes of hPRLR cluster sizes occur slowly and more subtly.

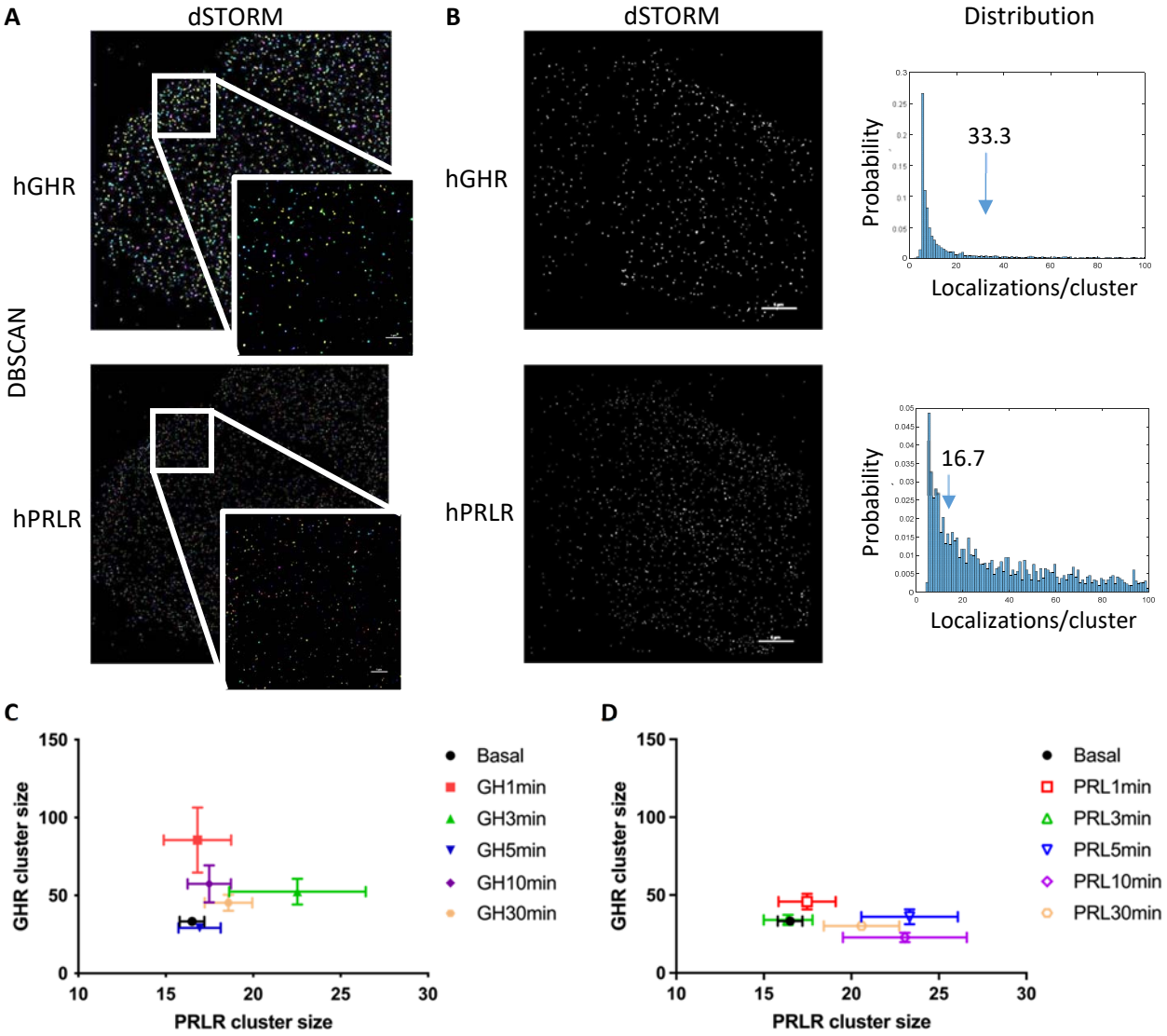

Fig. 3. GH/PRL stimulation induces a redistribution of hGHR and hPRLR clusters. **(A)** Sample dSTORM images and application of DBSCAN to identify and measure clusters (scale bar, 1 µm). **(B)** Left panels: Representative dSTORM images of hGHR (top) and hPRLR (bottom) on the T47D cell surface in resting state (scale bar, 5 µm). Brightness was increased by 40% for better visibility. Right panels: The corresponding histograms of the relative frequencies of localizations. **(C, D)** The medians of hGHR and hPRLR cluster sizes following GH (C) and PRL (D) treatment are summarized in these plots. The x-axis and y-axis represent hPRLR and hGHR cluster sizes, respectively. Data are collected from at least 6 cells from each group and displayed as median ± SE.

176 ## Spatial proximity of hGHR and hPRLR upon ligand stimulation

177 Nanoscale interactions of hGHR and hPRLR on the cell surface have yet to be well established. To evaluate
178 the extent of hGHR and hPRLR surface colocalization on T47D cells, we utilized proximity ligation assays
179 (PLAs). In PLAs, a positive signal appears only when two target proteins are in proximity (<40 nm). Notably,
180 individual treatment with GH or PRL for 5 min decreased the PLA signal observed in untreated cells by
181 34.4% and 28.1%, respectively (Fig. 4A), suggesting either ligand caused a reduction in the total number
182 of colocalized hGHR and hPRLR clusters. To further validate these observations, we calculated the ratio of
183 colocalized clusters in dSTORM images. Treatment with GH or PRL for 1 min reduced the proportion of
184 colocalized clusters by nearly 50% (Fig. 4B and 4C). To analyze their compositions, we plotted 3D
185 distributions for the colocalized clusters after ligand treatments (Fig. S1A and S1B). The probability of
186 observing co-localized clusters with numbers of hGHR and hPRLR that fall into certain bins is identified by
187 color and by the height of the bar on the z-axis. Following GH treatment for 1 min and 3 min, the number
188 of smallest clusters decreased, and the number of medium-sized clusters increased, suggesting a shift of
189 the bivariate distribution of co-localized cluster sizes toward medium-sized clusters (Fig. S1A). The
190 distribution of colocalized clusters after 5 min of GH treatment is similar to that at the basal state. In
191 contrast, after treatment with PRL for 3 min or more, the number of medium to large-sized clusters,
192 majoritarily containing either GHR or PRLR, decreased, while the number of smallest clusters increased
193 (Fig. S1B). Together, these results demonstrate that hGHR and hPRLR are spatially accessible to each other
194 and form receptor complexes on the T47D cell surface and that the nature of these complexes changes
195 differentially depending on the stimulating ligand.

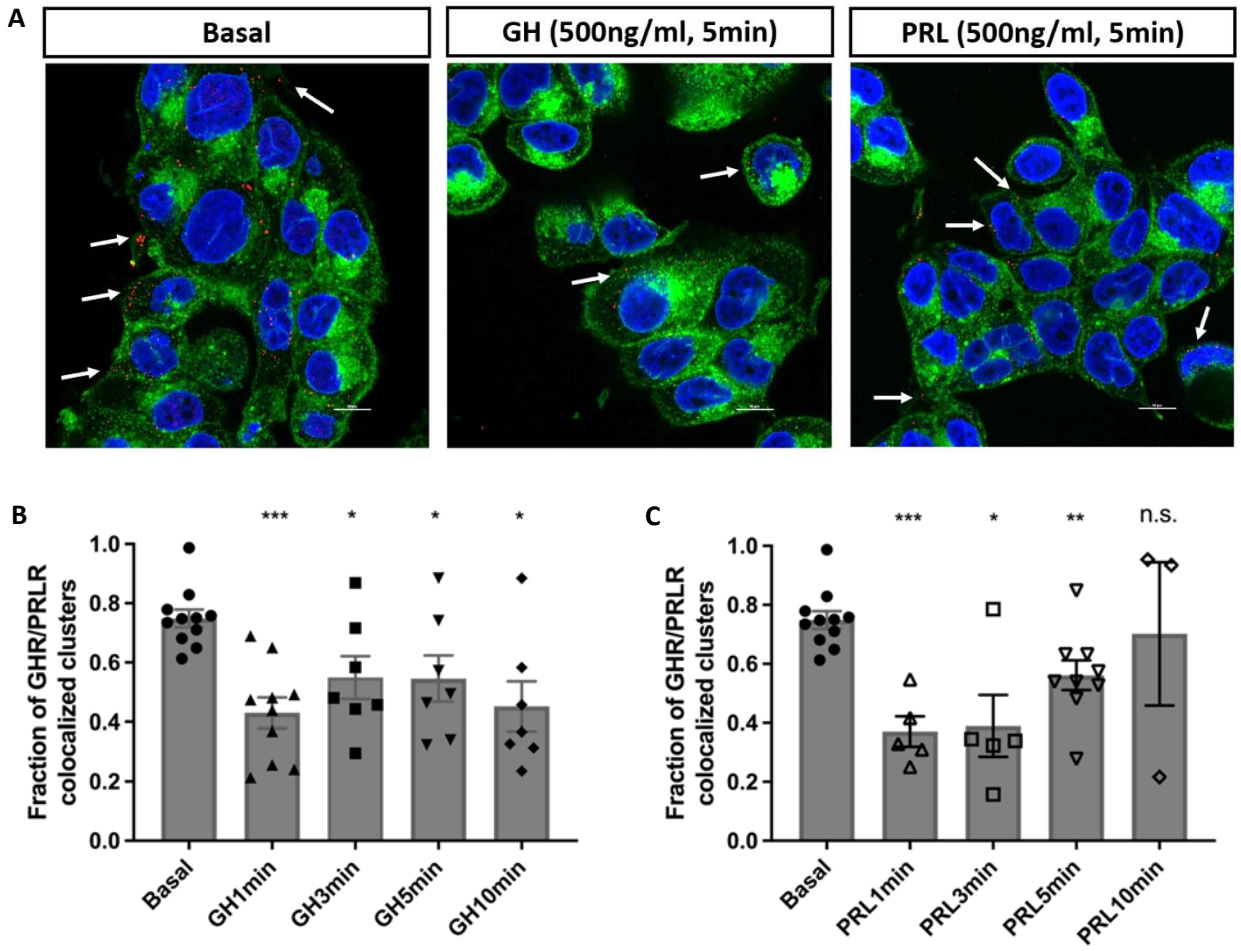

Fig. 4. Spatial proximity of hGHR and hPRLR upon ligand stimulation. **(A)** Proximity ligation assays were performed in T47D cells (scale bar, 10 µm). Here we show representative confocal microscopy images of T47D cells at resting and ligand stimulation conditions. The PLA signal (red dots) corresponds to hGHR and hPRLR complexes, wheat germ agglutinin (green staining) corresponds to the cell membrane, and DAPI (blue staining) corresponds to cell nuclei. **(B, C)** hGHR and hPRLR colocalization changes in T47D cell surface following 500 ng/ml GH (B) or PRL (C) treatment. Each data point represents a ratio of clusters, which contain both hGHR and hPRLR, to the total clusters on the cell surface. Data are displayed as mean ± SE. * (P<0.05), ** (P<0.01), and *** (P<0.001) indicate the statistical significance in comparison with Basal and are calculated by a two-tailed t-test assuming unequal variance.

Reduction of hGHR induced by PRL on the cell surface is dependent on the presence of PRLR

PRL strongly binds PRLR but not GHR. Yet, PRL induces a decrease of hGHR on the surface of cells expressing both hGHR and hPRLR. Thus, we sought to investigate the effect of PRL on hGHR in the absence of hPRLR. We utilized CRISPR/Cas9 technology to generate hPRLR knockout T47D cells (termed $T47D_{\Delta PRLR}$).

212 In addition, to evaluate isolated hPRLR responses to ligands, we also generated hGHR knockout T47D cells
213 (termed $T47D_{\Delta GHR}$). Immunoblot analysis with specific GHR and PRLR antibodies confirmed the absence of
214 hPRLR in $T47D_{\Delta PRLR}$ cells and hGHR in $T47D_{\Delta GHR}$ cells (Fig 5A). Similar to our results with parental T47D cells,
215 GH treatment of $T47D_{\Delta PRLR}$ cells rapidly reduces the density of surface hGHR, suggesting that hPRLR need
216 not be present to allow this GH-induced effect (Fig 5B). However, contrary to findings in parental T47D
217 cells, PRL treatment of $T47D_{\Delta PRLR}$ cells fails to modulate hGHR surface density (Fig 5C). Like parental T47D
218 cells, treatment of $T47D_{\Delta GHR}$ cells with GH (Fig 5D) or PRL (Fig 5E) yielded increased hPRLR surface
219 localizations. Thus, we conclude that the PRL-induced decrease of hGHR in T47D cells is dependent on the
220 presence of hPRLR, but the ability of both GH and PRL to increase surface hPRLR in T47D cells is
221 independent of hGHR's presence.

222 To extend our observations, we next examined the GH and PRL responses in a cellular reconstitution
223 system: γ2A-JAK2 [55-57] is a human JAK2-deficient fibrosarcoma cell line reconstituted with JAK2 that
224 stably expresses JAK2 but lacks hGHR and hPRLR. To independently study the role of each receptor in this
225 setting, we used our previously generated stable transfectants of γ2A-JAK2 cells that harbor either hGHR
226 or hPRLR [58] and verified the presence of the indicated receptor by immunoblotting (Fig. 5F). Consistent
227 with the observation in $T47D_{\Delta PRLR}$ cells, γ2A-JAK2-hGHR cells responded with a loss of surface hGHR density
228 to GH stimulation but not to PRL stimulation (Fig. 5G). Interestingly, as in $T47D_{\Delta GHR}$ cells, treatment of γ2A-
229 JAK2-hPRLR cells with either GH or PRL (Fig. 5H) promotes increased surface hPRLR. Thus, our findings in
230 both cell systems suggest that hPRLR-hGHR interaction, direct or indirect, is indispensable for PRL-induced
231 but not for GH-induced loss of surface hGHR.

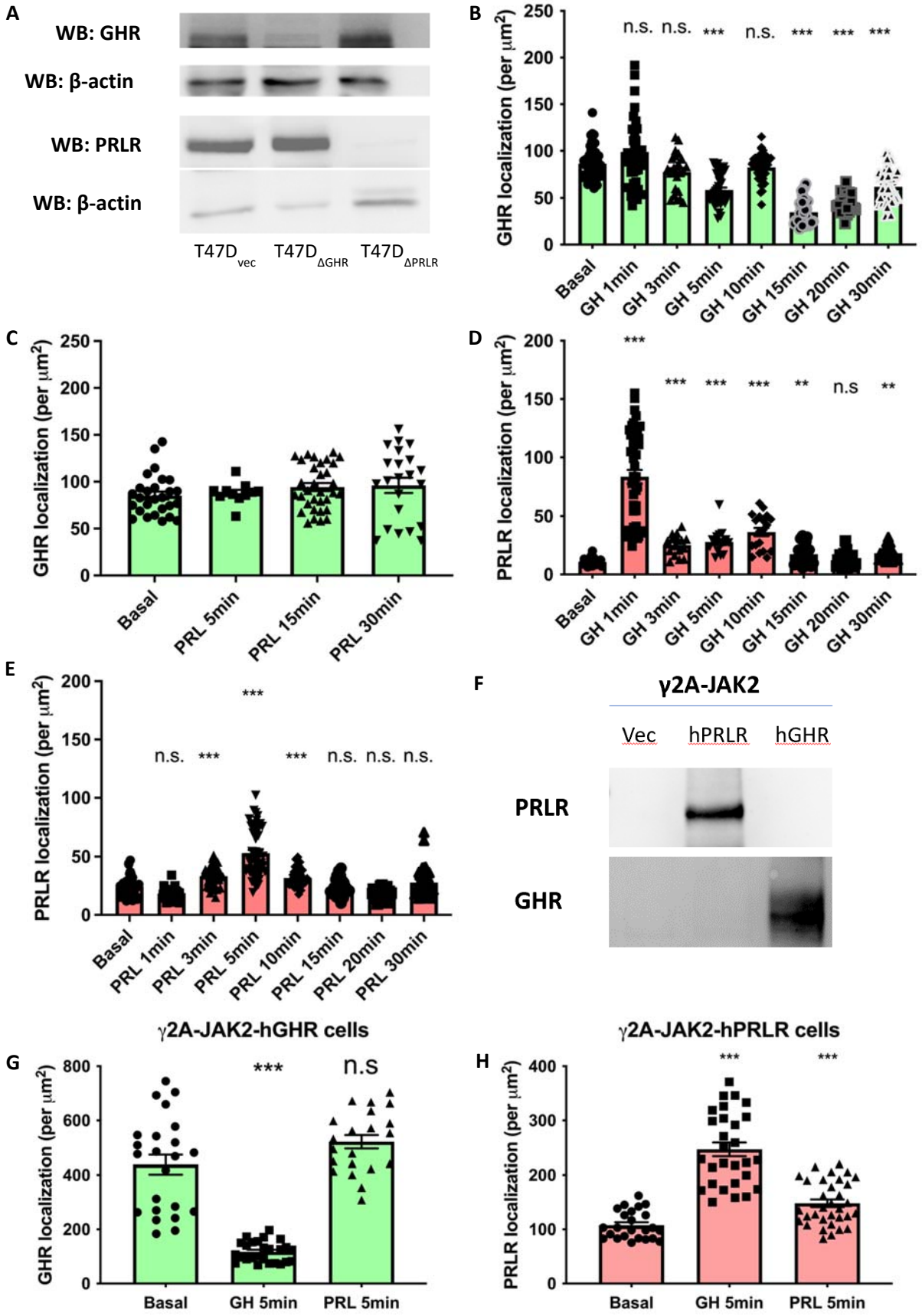
A
WB: GHR
WB: β-actin
WB: PRLR
WB: β-actin
T47D vec
T47D ΔGHR
T47D ΔPRLR
B
GHR localization (per μm²)
n.s. n.s. *** n.s. *** *** ***
Basal
GH 1min
GH 3min
GH 5min
GH 10min
GH 15min
GH 20min
GH 30min
C
GHR localization (per μm²)
Basal
PRL 5min
PRL 15min
PRL 30min
D
PRLR localization (per μm²)
*** *** *** *** ** n.s **
Basal
GH 1min
GH 3min
GH 5min
GH 10min
GH 15min
GH 20min
GH 30min
E
PRLR localization (per μm²)
n.s. *** *** n.s. n.s. n.s.
Basal
PRL 1min
PRL 3min
PRL 5min
PRL 10min
PRL 15min
PRL 20min
PRL 30min
F
γ2A-JAK2
Vec
hPRLR
hGHR
PRLR
GHR
γ2A-JAK2-hGHR cells
G
GHR localization (per μm²)
*** n.s
Basal
GH 5min
PRL 5min
γ2A-JAK2-hPRLR cells
H
PRLR localization (per μm²)
*** ***
Basal
GH 5min
PRL 5min

232

233 **Fig. 5.** PRL-induced reduction of hGHR on the cell surface depends on the presence of PRLR. **(A)** Detergent
234 cell extracts of $T47D_{vec}$, $T47D_{\Delta GHR}$, and $T47D_{\Delta PRLR}$ were analyzed by immunoblotting with anti-$GHR_{cyt\text{-}AL47}$,
235 anti-$PRLR_{cyt,}$ and anti-β-actin antibodies. **(B)** In $T47D_{\Delta PRLR}$, GH (500 ng/ml) induces downregulation of hGHR
236 localizations on the cell surface, while **(C)** PRL does not change hGHR localizations. **(D, E)** In $T47D_{\Delta GHR}$ cells,
237 GH (D) and PRL (E) incite an increase of hPRLR on the cell surface. Data are displayed as mean ± SE. *
238 (P<0.05), ** (P<0.01), and *** (P<0.001) indicate the statistical significance in comparison with Basal and
239 are calculated by a two-tailed t-test assuming unequal variance. **(F)** γ2A-JAK2 cells with stable expression
240 of hGHR or hPRLR. Detergent extracts were resolved by SDS-PAGE and immunoblotted with anti-$GHR_{cyt\text{-}}$
241 $_{AL47}$ and anti-$PRLR_{cyt\text{-}AL84}$ antibodies. **(G, H)** Serum-starved γ2A-JAK2-hGHR cells (G) or γ2A-JAK2-hPRLR cells
242 (H) were treated with GH (500 ng/ml) or PRL (500 ng/ml) for 5 min. Localizations of hGHR in γ2A-JAK2-
243 hGHR cells were decreased after GH treatment while remaining the same after PRL treatment compared
244 to the basal state. Localizations of hPRLR in γ2A-JAK2-hPRLR cells were increased by GH or PRL treatment.
245 Data are displayed as mean ± SE. * (P<0.05), ** (P<0.01), and *** (P<0.001) denote the statistical
246 significance in comparison with Basal and are calculated by a two-tailed t-test assuming unequal variance.

247

248

Box 1 region in hPRLR contributes to PRL-induced GHR downregulation

The hPRLR-dependent PRL-induced hGHR downregulation indicates that hPRLR can modulate the density of hGHR on the cell surface in response to PRL. To investigate this interaction, we generated a set of truncation or deletion mutants of hPRLR: (1) hPRLR-tr292, which truncates the intracellular domain of hPRLR distal to the membrane-proximal intracellular domain box 1 element; (2) hPRLR-tr238, which contains only 4 amino acids of the proximal intracellular domain and does not include box 1; and (3) hPRLR-Δbox1, in which the box 1 region (243aa-251aa) is internally deleted (shown in Fig. 6A). Expression of hPRLR-tr292, hPRLR-tr238, and hPRLR-Δbox1, as well as wild-type hPRLR, was detected by immunoblotting using monoclonal antibodies targeting the ECD of PRLR ($mAb_{ext-1.48}$). Since hPRLR-tr238 contains only 4aa in its ICD, no immunoblot signal was detected using a polyclonal antibody (Ab_{AL-84}) targeting the hPRLR ICD. In contrast, the expression of hPRLR-tr292 was easily detected by Ab_{AL-84} (Fig. 6B). We then transiently transfected each hPRLR construct into the γ2A-JAK2-hGHR cells, which stably express hGHR, and analyzed the changes of cell surface hGHR localizations. In cells expressing wild-type hPRLR (hPRLR-WT), the localizations of hGHR significantly decreased 3 min post-exposure to GH and PRL (Fig. 6C). Similarly, under the same treatment, in cells expressing hPRLR-tr292, the localization of hGHR on the cell membrane was reduced in response to each ligand (Fig. 6D). However, in hPRLR-tr238-expressing cells, the localization of hGHR was diminished by GH stimulation but slightly increased by PRL stimulation (Fig. 6E). To further investigate the role of the box1 region for hGHR and hPRLR functional interaction, we studied hPRLR-Δbox1 expressing cells and found that upon PRL treatment, hGHR localizations did not decrease on the cell surface (Fig. 6F). As a negative control, we transfected the cells with vector (pcDNA3.1). hGHR localization decreased upon GH stimulation but remained at basal levels upon PRL stimulation (Fig. 6G). In addition, in hPRLR-ΔBox1 and hGHR expressing cells, the JAK2 and STAT5 tyrosine phosphorylation levels were assessed in response to GH and PRL stimulations. Treatment of 500ng/ml GH induces a dramatic increase in both JAK2 and STAT5 phosphorylation. In contrast, 500ng/ml PRL treatment does not cause JAK2 or STAT5 phosphorylation (Fig. 6H), consistent with PRLR Box1 being required for effective coupling of PRL occupancy of PRLR to activation of JAK2 and phosphorylation of STAT5 and the inability of PRL to signal via GHR.

Next, we analyzed colocalization in each group. In the resting state, the ratios of GHR-PRLR-colocalization clusters are relatively higher in hPRLR-WT- and hPRLR-tr292-expressing cells in comparison with hPRLR-tr238- and hPRLR-ΔBox1-expressing cells (Fig. 6I). This suggests that the box 1 region in hPRLR plays a critical role in stabilizing the hGHR-hPRLR complexes in the basal state.

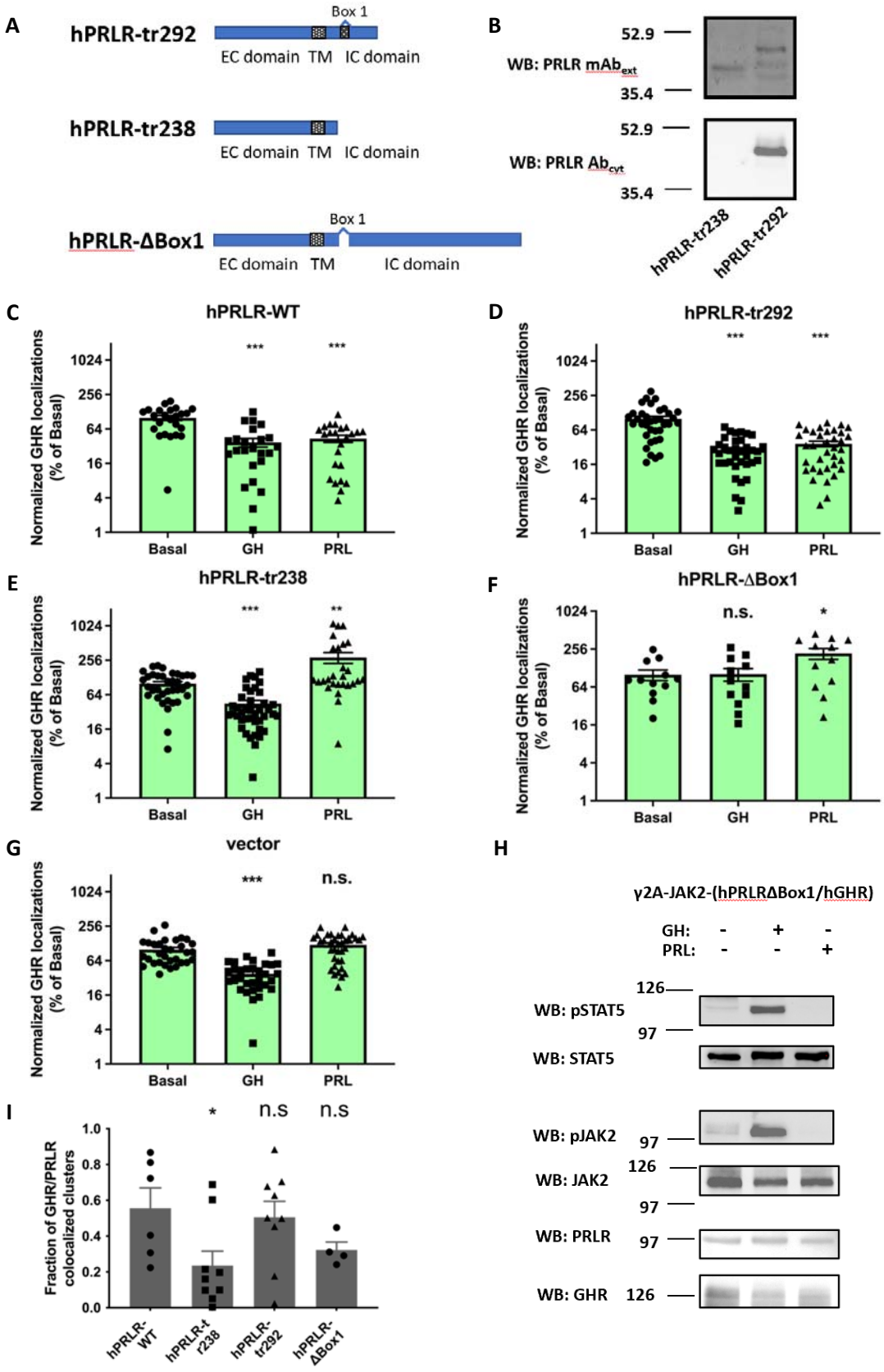
A
hPRLR-tr292
Box 1
EC domain TM IC domain
hPRLR-tr238
EC domain TM IC domain
hPRLR-ΔBox1
Box 1
EC domain TM IC domain
B
52.9
WB: PRLR mAb$_{ext}$
35.4
52.9
WB: PRLR Ab$_{cyt}$
35.4
hPRLR-tr238
hPRLR-tr292
C
hPRLR-WT
Normalized GHR localizations (% of Basal)
1024
256
64
16
4
1
***
***
Basal
GH
PRL
D
hPRLR-tr292
***
***
E
hPRLR-tr238
***
**
F
hPRLR-ΔBox1
n.s.
*
G
vector
***
n.s.
H
γ2A-JAK2-(hPRLRΔBox1/hGHR)
GH: - + -
PRL: - - +
126
WB: pSTAT5
97
WB: STAT5
WB: pJAK2
97
126
WB: JAK2
97
WB: PRLR
97
WB: GHR
126
I
Fraction of GHR/PRLR colocalized clusters
1.0
0.8
0.6
0.4
0.2
0.0
*
n.s
n.s
hPRLR-WT
hPRLR-tr238
hPRLR-tr292
hPRLR-ΔBox1

285

286 **Fig. 6.** Box 1 region in hPRLR contributes to PRLR-induced GHR downregulation. **(A)** Diagrams of employed
287 mutant hPRLR variants with truncations or deletion in the intracellular domain. ECD, extracellular domain;
288 TMD, transmembrane domain; ICD, intracellular domain. **(B)** γ2A-JAK2-hGHR cells were transiently
289 transfected with hPRLR-tr292 and hPRLR-tr238. Cell extracts were resolved by SDS-PAGE and blotted with
290 anti-PRLR $mAb_{ext-1.48}$ and anti-$PRLR_{cyt-AL84}$. **(C-G)** γ2A-JAK2-hGHR cells were transfected with (C) wild-type
291 hPRLR (hPRLR-WT), (D) hPRLR truncated at 292 aa (hPRLR-tr292), (E) hPRLR truncated at 238 aa (hPRLR-
292 tr238), (F) hPRLR with box1 motif deleted (hPRLR-ΔBox1) and (G) vector pcDNA3.1 (vector). Transfected
293 cells were imaged by dSTORM microscopy and analyzed using the DBSCAN algorithm. The density of hGHR
294 localizations on the cell surface was calculated. Each data point represents the density of hGHR in a cell
295 surface area of size 6.25 µm X 6.25 µm. Data are collected from at least 6 cells (4 ROIs per cell) from each
296 group, and values are displayed as mean ± SE (from three independent experiments). Data are normalized
297 such that the basal is 100%. * (P<0.05), ** (P<0.01), and *** (P<0.001) denote the statistical significance
298 in comparison with Basal and are calculated by a two-tailed t-test assuming unequal variance. **(H)**
299 Detergent cell extracts of hPRLR-ΔBox1 and hGHR-expressing cells were analyzed by immunoblotting.
300 After 5 hrs. starvation, cells were treated with GH (500 ng/ml) or PRL (500 ng/ml) for 10 min. In each
301 experiment, the average Basal value is considered 100%. **(I)** Fraction of GHR/PRLR colocalized clusters. In
302 the resting state, the colocalization ratio is significantly lower for cells expressing hPRLR-tr238 than for
303 those expressing hPRLR-WT. Each data point represents the ratio of the number of clusters, which contain
304 both hGHR and hPRLR, to the total number of clusters on the cell surface. Data are displayed as mean ±
305 SE. * (P<0.05) indicates statistical significance in comparison with WT and is calculated by a two-tailed t-
306 test assuming unequal variance (all bars without an asterisk are not significant).

307

308 Box 1 region in hGHR plays an essential role in regulating PRLR and GHR interaction

309 From our observations (Fig. 6), we concluded that the JAK2 binding site, i.e., the box 1 region, in hPRLR is
310 required for PRL-induced hGHR down-regulation from the cell surface. To further assess whether the JAK2
311 binding site on hGHR is also essential, we generated hGHR-ΔBox1, in which the box 1 region (297aa –
312 305aa) was deleted (Fig. 7A). In cells expressing both hGHR-ΔBox1 and hPRLR we observed that GH does
313 not alter the hGHR-ΔBox1 localizations on the cell surface, while PRL slightly increases hGHR-ΔBox1
314 localizations (Fig. 7B). Together, these results re-affirm that binding of JAK2 to hGHR is also required for
315 hPRLR-mediated regulation of hGHR availability on the cell surface.

316

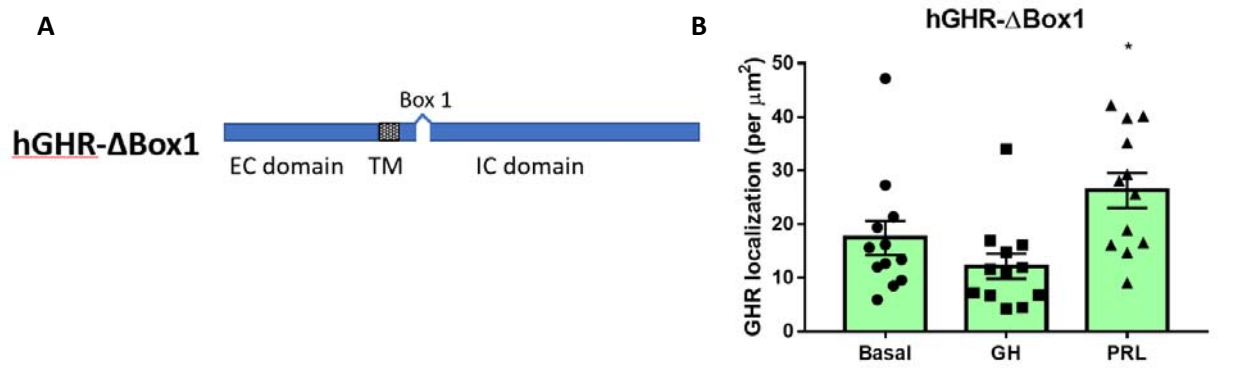

317 **Fig. 7.** Box 1 region in hGHR also plays an important role in PRLR and GHR interaction. **(A)** Diagram of
318 hGHR-ΔBox1 showing the deleted box 1 region in the intracellular domain of hGHR. **(B)** γ2A-JAK2-hPRLR
319 cells were transfected with hGHR-ΔBox1. Transfected cells were imaged by dSTORM microscopy and
320 analyzed using DBSCAN. The density of hGHR localizations on the cell surface was calculated. Each data
321 point represents the density of hGHR in a cell surface area of size 6.25 µm X 6.25 µm. Data are collected
322 from at least 6 cells for each group and displayed as mean ± SE. * (P<0.05), ** (P<0.01), and ***(P<0.001)
323 indicate the statistical significance in comparison with Basal and are calculated by a two-tailed t-test
324 assuming unequal variance.

325

326 Materials and Methods:

327 Materials:

328 Common reagents were purchased from Sigma Aldrich Corp. (St. Louis, MO) unless otherwise noted. Fetal
329 bovine serum was purchased from Atlanta Biologicals (Lawrenceville, GA). Cell culture medium,
330 penicillin/streptomycin and trypsin were purchased from Corning (Corning, NY). Recombinant hGH was
331 kindly provided by Eli Lilly & Co. (Indianapolis, IN). Recombinant human PRL was obtained from the
332 National Hormone and Pituitary Program.

333 Antibodies:

334 Polyclonal anti-$GHR_{cytAL-47}$ (1:1000) against the intracellular domain of GHR described previously [59] was
335 used as the primary antibody for western blot analysis. Monoclonal anti-$GHR_{ext-mAb}$ (1:1000) against the
336 extracellular S2 domain of GHR [60] and monoclonal anti-$PRLR_{ext-mAb}$ against the extracellular S2 domain
337 of human PRLR [47] was used for microscopy. A detailed description is provided in the references. The
338 following secondary antibodies were used: Alexa Fluor 568 goat anti-mouse IgG1 (Invitrogen #A-21124)
339 (1:1000), Alexa Fluor 647 goat anti-mouse IgG2b (Invitrogen #A-21242) (1:1000), Alexa Fluor 647 goat
340 anti-mouse IgG1 (Invitrogen #A-21240) (1:1000) and Alexa Fluor 568 goat anti-mouse IgG2b (Invitrogen #
341 A-21144) (1:1000).

342 Cloning and constructs:

343 The human GHR cDNA in pcDNA1 was a generous gift from R. Ross (University of Sheffield, Sheffield, UK).
344 The human PRLR cDNA in pEF/V5/HIS was generously provided by C. Clevenger (Virginia Commonwealth

University, Richmond, VA). hPRLR-tr238 and hPRLR-tr292 were generated by amplifying with external primers containing EcorI site and a stop codon with XhoI site after the sequence of 238 or 292 amino acid, respectively. hPRLR-ΔBox1, and hGHR-Δbox1 were generated by overlap extension polymerase chain reaction (PCR) with associated primers and cloned into pcDNA3.1(+) vector.

Cell culture and transfections:

Human T47D breast cancer cells were purchased from American Type Culture Collection (Manassas, VA). Cells were maintained in RPMI 1640 medium supplemented with 10% fetal bovine serum (FBS), 100 units/ml penicillin and 100 μg/ml streptomycin in a humidified atmosphere of 5% CO2 and 95% air at 37 ℃.

γ2A-JAK2 cells were generated by transfection of γ2A cells [55] with pcDNA3.1(+)/zeo-JAK2 and maintained in culture, as described previously [56, 57]. The generation of γ2A-JAK2-GHR and γ2A-JAK2-PRLR cells has been previously described [58].

Transient expression of receptors was achieved by using Lipofectamine LTX Plus (Invitrogen), transfecting 0.3 pmol plasmid DNA per 6-cm^2 dish.

Western blot

Cells were serum starved for 5 hours and treated with 500 ng/ml GH or 500 ng/ml PRL at 37 °C for 10 min. Stimulations were terminated by washing the cells with ice-cold phosphate-buffered saline supplemented with 0.4 mM sodium orthovanadate. Cells were lysed in lysis buffer for 30 min at 4°C. Then cell lysates were centrifuged at 15,000 g for 10 min at 4°C. The protein extracts (supernatant) along with SDS sample buffer were resolved by SDS-PAGE.

Sample preparation for imaging:

Cells were seeded into either eight well #1.5 coverslip bottom dishes (Ibidi) or 25 mm #1.5 coverslips (Electron Microscopy Sciences). Cells were serum starved for 5 hours, then treated with GH (500 ng/ml), PRL (500 ng/ml) at 37 °C for the indicated time. Then the cells were washed with PBS three times and fixed with 4% PFA (paraformaldehyde) for 10 min. After multiple washes with PBS, cells were blocked with 5% normal horse serum, 5% normal goat serum, 1% BSA for 30 min. Lastly, cells were incubated in primary antibody for 3h and secondary antibody for 70 min at 37°C.

dSTORM imaging and data analysis

dSTORM experiments were conducted on an inverted Nikon Ti2 N-STORM microscope equipped with a 100 X 1.49 NA oil immersion objective (Nikon, Japan), 488 and 647 nm lasers, and an iXon DU-897 ultra EMCCD camera (Andor, Oxford Instruments). The dSTORM imaging buffer included glucose oxidase (Sigma, St Louis, Missouri), glucose (Sigma, St Louis, Missouri), catalase (Roche, Penzberg, Germany), and β-mercaptoethanol (Sigma, St Louis, Missouri). The cell membrane was focused using TIRF excitation, which selectively images within 100-150 nm of the cell membrane, making it an excellent method to study surface distribution of membrane proteins. For dual color STORM imaging, the sample was illuminated with 561nm or 647 nm lasers alternatively and 40,000 frames of images were acquired per channel. The chromatic offset associated with the different acquisition wavelengths was corrected using 0.1 μm microspheres [61, 62].

383 dSTORM images were reconstructed using the built-in STORM module in NIS-Elements (Nikon). The
384 localizations list was exported and further analyzed in *Matlab*. In particular, for the DBSCAN cluster
385 analysis, we employed Clus-DoC directly on the list of localizations, utilizing the parameters of a minimum
386 of 4 neighbors within a cluster radius of 20nm [63].

387 Statistical analysis

388 Imaging and biochemical experiments were carried out at least three times to ensure reproducibility. Data
389 were analyzed using unpaired, two-tailed t-tests. *Prism* software was used for statistical analysis
390 (GraphPad Inc, USA). Data are presented as means ± s.e.m.

391

392 Discussion:

393 The non-ligand-bound states of hGHR and hPRLR have been extensively investigated. Pre-
394 homodimerization of hGHR and hPRLR has been reported using structural and biochemical methods [35,
395 64-67]. At the same time, a recent study supports the notion that GHR, at physiological densities, exists
396 as monomers on the cell surface and becomes activated by a ligand-induced dimerization [68]. The current
397 study uses a highly precise and sensitive single-molecule localization microscopy approach to study the
398 formation of hGHR and hPRLR nanoclusters and the cell surface receptor availability. Our super-resolution
399 images reveal that in human T47D breast cancer cells and the γ2A-JAK2 cell exogenous expression system,
400 the cluster size of hGHR and hPRLR in the basal state range from a few localizations per cluster up to a
401 thousand localizations per cluster.

402 With GH or PRL treatment, the number of hGHR on both T47D and γ2A-JAK2 cell surfaces is decreased,
403 indicating the removal of surface hGHR. Moreover, the distribution curve of hGHR shifts toward larger
404 cluster sizes (Fig. 3), suggesting a ligand-induced aggregation of receptors. In turn, hPRLR numbers
405 dramatically increase on the cell surface in response to ligand stimulation. The newly presented hPRLR
406 clusters may impact the distribution of cluster sizes, which may explain why the median of hPRLR cluster
407 sizes does not change much with ligand treatment.

408 Our PL assay data indicate that distances between hGHR and hPRLR are small (less than 40nm). This
409 implies that hGHR and hPRLR form co-localized clusters in unstimulated states, suggesting hGHR and
410 hPRLR are physically accessible to one other. With GH stimulation, the fraction of co-localized receptors
411 is decreased. Given that GH treatment enhances the coimmunoprecipitation of total cellular hGHR and
412 hPRLR [45], the decrease in co-localized surface receptors can likely be attributed to removing co-localized
413 receptors from the cell surface.

414 It is well documented that hPRLR is engaged by both PRL and GH, while hGHR only responds to GH [36,
415 38, 39]. Unexpectedly, we found that PRL induces a down-regulation of cell surface hGHR in cells that co-
416 express hGHR and hPRLR (Fig. 2), indicating that hPRLR directly or indirectly interacts with hGHR.
417 Interestingly, PRL was unable to induce hGHR down-regulation in cells either lacking hPRLR or expressing
418 hPRLR without its Box1 region (hPRLR-tr238 or hPRLR-ΔBox1), suggesting that JAK2 and PRLR association
419 is required for hGHR-hPRLR interaction that in turn allows PRL-induced hGHR downregulation. Notably,
420 previous work showed that GHR and JAK2 association is necessary for JAK2 to stabilize cell surface GHR
421 and inhibit constitutive GHR down-regulation [57]. Furthermore, single-particle tracking studies showed
422 that, in the presence of JAK2, a higher level of ligand-induced dimerization of GHR was observed [68].

423 Moreover, JAK2 with intact kinase activity is required for GH-induced GHR down-regulation [57]. Similarly,
424 the box1 region of PRLR also associates with JAK2, and deletion or modulation of the last proline residue
425 of box1 abrogates PRLR function [69]. Collectively, these findings suggest that the box1 regions in hGHR
426 and hPRLR play a crucial role in the transduction of the individual signaling cascades and hGHR-hPRLR
427 association.

428 Here we found that, in the resting state, the degree of hGHR-hPRLR colocalization is higher in cells
429 expressing hPRLR with the box1 motif. This suggests JAK2 may not only stabilize GHR but also support the
430 formation of hGHR-hPRLR-containing clusters. Previously, it has been suggested that such clusters are
431 comprised of hGHR homodimers and hPRLR homodimers that together form (hGHR-hGHR) – (hPRLR-
432 hPRLR) hetero-multimers or higher order oligomers [46]. Indeed, because the intracellular domains (ICD)
433 of both hGHR and hPRLR are highly disordered, the flexibility of their ICDs may provide room for recruiting
434 JAK2 and stabilizing the hGHR-hPRLR association [70, 71]. Moreover, a study of the crystal structure of
435 erythropoietin receptor (EPOR) and leptin receptor (LEPR), which also belong to the class I cytokine
436 receptor family, revealed recently that JAK2/EPOR and JAK2/LEPR complexes contained four JAK2 and
437 four EPOR or LEPR molecules, respectively [72]. Hence, it is possible that hGHR-hGHR homodimers and
438 hPRLR-hPRLR homodimers form complexes in a similar fashion (Fig. 8). We propose that this JAK2/Box1-
439 mediated interaction of receptors is not limited to hGHR and hPRLR but may generalize to other receptors
440 of the class I cytokine receptor family. We note, however, that determinants within particular receptors
441 (perhaps residing in their extracellular and/or transmembrane domains) and their intracellular JAK2
442 association domains may facilitate, to varying degrees, their propensity to form multimeric aggregates.
443 GHR and PRLR, for example, may tend to do so more avidly with each other than either one does with
444 other cytokine receptors. Additional studies are required to determine and understand the modes and
445 functions of the hGHR-hPRLR association.

446 Lastly, hPRL/hPRLR-mediated downregulation of surface hGHR may be a relevant factor in the observed
447 anti-tumor effect of PRLR signaling, especially in triple-negative breast cancer (TNBC) expressing PRLR but
448 lacking other interfering hormone receptors. As previously shown, the TNBC cell lines MDA-MB-231 and
449 MDA-MB-453 show significantly increased GHR [15] while expressing no or only endogenous levels of
450 PRLR, respectively [28]. PRL treatment significantly decreased cell viability and invasive capacity of MDA-
451 MB-231 cells following the restoration of PRLR expression. In MDA-MB-453 cells, PRL caused a significant
452 reduction in cell viability. A xenograft model with inoculated MDA-MB-453 cells confirmed the growth
453 inhibitory effect of PRL treatment *in vivo*, suggesting PRLR expression as an indicator of a favorable
454 prognosis. Future research will have to investigate our hypothesis that PRLR-mediated downregulation of
455 surface GHR contributed to the anti-tumoral effect of PRL treatment in PRLR-positive TNBC.

456

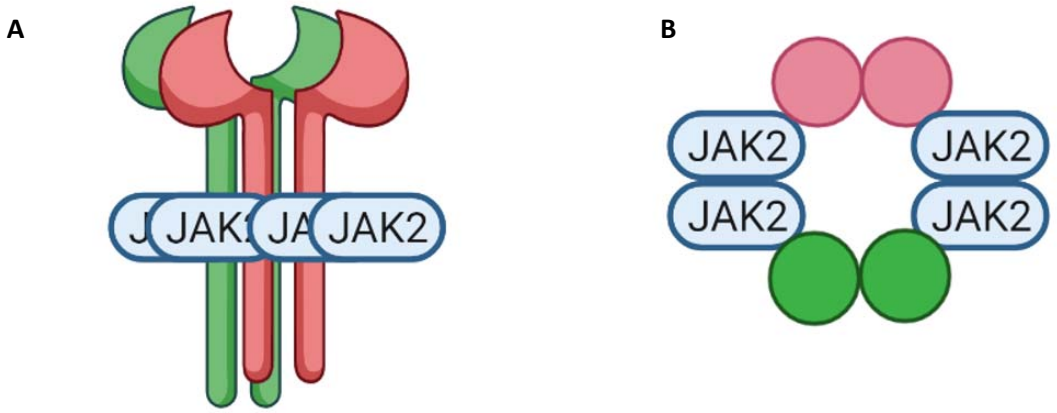

457

458 **Fig. 8**. Model of JAK2 stabilizing GHR-GHR and PRLR-PRLR heteromers. **(A)** Schematic representation of
459 GHRs homodimer and PRLRs homodimer form a heteromer, which contains two PRLRs (red), two
460 GHRs(green), and four JAK2(blue). **(B)** A top view of the JAK2/PRLR/GHR multimer.

461

462 Reference:

463 1. Isaksson, O.G., S. Eden, and J.O. Jansson, *Mode of action of pituitary growth hormone on target*
464 *cells.* Annu Rev Physiol, 1985. **47**: p. 483-99.
465 2. Moller, N. and J.O. Jorgensen, *Effects of growth hormone on glucose, lipid, and protein metabolism*
466 *in human subjects.* Endocr Rev, 2009. **30**(2): p. 152-77.
467 3. Brooks, C.L., *Molecular mechanisms of prolactin and its receptor.* Endocr Rev, 2012. **33**(4): p. 504-
468 25.
469 4. Gonzalez-Lucano, L.R., et al., *Increased expression of the prolactin receptor is associated with*
470 *malignant laryngeal tumors.* Exp Ther Med, 2012. **3**(4): p. 603-607.
471 5. Ascencio-Cedillo, R., et al., *Prolactin and prolactin receptor expression in cervical intraepithelial*
472 *neoplasia and cancer.* Pathol Oncol Res, 2015. **21**(2): p. 241-6.
473 6. Harris, J., et al., *Prolactin and the prolactin receptor: new targets of an old hormone.* Ann Med,
474 2004. **36**(6): p. 414-25.
475 7. Asad, A.S., et al., *The role of the prolactin receptor pathway in the pathogenesis of glioblastoma:*
476 *what do we know so far?* Expert Opin Ther Targets, 2020. **24**(11): p. 1121-1133.
477 8. Sethi, B.K., G.V. Chanukya, and V.S. Nagesh, *Prolactin and cancer: Has the orphan finally found a*
478 *home?* Indian J Endocrinol Metab, 2012. **16**(Suppl 2): p. S195-8.
479 9. Boguszewski, C.L. and M. Boguszewski, *Growth Hormone's Links to Cancer.* Endocr Rev, 2019.
480 **40**(2): p. 558-574.
481 10. Strous, G.J., et al., *Growth Hormone Receptor Regulation in Cancer and Chronic Diseases.* Front
482 Endocrinol (Lausanne), 2020. **11**: p. 597573.
483 11. Chhabra, Y., M.J. Waters, and A.J. Brooks, *Role of the growth hormone-IGF-1 axis in cancer.* Expert
484 Rev Endocrinol Metab, 2011. **6**(1): p. 71-84.
485 12. Clevenger, C.V. and H. Rui, *Breast Cancer and Prolactin - New Mechanisms and Models.*
486 Endocrinology, 2022. **163**(10).
487 13. Shemanko, C.S., *Prolactin receptor in breast cancer: marker for metastatic risk.* J Mol Endocrinol,
488 2016. **57**(4): p. R153-R165.
489 14. Goffin, V., *Prolactin receptor targeting in breast and prostate cancers: New insights into an old*
490 *challenge.* Pharmacol Ther, 2017. **179**: p. 111-126.
491 15. Zhu, X., et al., *Growth hormone receptor promotes breast cancer progression via the*
492 *BRAF/MEK/ERK signaling pathway.* FEBS Open Bio, 2020. **10**(6): p. 1013-1020.
493 16. Subramani, R., et al., *Role of Growth Hormone in Breast Cancer.* Endocrinology, 2017. **158**(6): p.
494 1543-1555.
495 17. Xu, J., et al., *The role of prolactin receptor in GH signaling in breast cancer cells.* Mol Endocrinol,
496 2013. **27**(2): p. 266-79.
497 18. Gebre-Medhin, M., et al., *Growth hormone receptor is expressed in human breast cancer.* Am J
498 Pathol, 2001. **158**(4): p. 1217-22.
499 19. Mertani, H.C., et al., *Cellular expression of growth hormone and prolactin receptors in human*
500 *breast disorders.* Int J Cancer, 1998. **79**(2): p. 202-11.
501 20. Kavarthapu, R., R. Anbazhagan, and M.L. Dufau, *Crosstalk between PRLR and EGFR/HER2 Signaling*
502 *Pathways in Breast Cancer.* Cancers (Basel), 2021. **13**(18).
503 21. Wang, L., et al., *Functional regulations between genetic alteration-driven genes and drug target*
504 *genes acting as prognostic biomarkers in breast cancer.* Sci Rep, 2022. **12**(1): p. 10641.
505 22. Liang, J., et al., *PRLR and CACNA2D1 Impact the Prognosis of Breast Cancer by Regulating Tumor*
506 *Immunity.* J Pers Med, 2022. **12**(12).

23. Fiorillo, A.A., et al., *The prolactin receptor transactivation domain is associated with steroid hormone receptor expression and malignant progression of breast cancer.* Am J Pathol, 2013. **182**(1): p. 217-33.
24. Schuler, L.A. and K.A. O'Leary, *Prolactin: The Third Hormone in Breast Cancer.* Front Endocrinol (Lausanne), 2022. **13**: p. 910978.
25. Swaminathan, G., B. Varghese, and S.Y. Fuchs, *Regulation of prolactin receptor levels and activity in breast cancer.* J Mammary Gland Biol Neoplasia, 2008. **13**(1): p. 81-91.
26. Hachim, I.Y., et al., *Prolactin Receptor Expression is an Independent Favorable Prognostic Marker in Human Breast Cancer.* Appl Immunohistochem Mol Morphol, 2016. **24**(4): p. 238-45.
27. Hachim, I.Y., et al., *A favorable role of prolactin in human breast cancer reveals novel pathway-based gene signatures indicative of tumor differentiation and favorable patient outcome.* Hum Pathol, 2016. **53**: p. 142-52.
28. Lopez-Ozuna, V.M., et al., *Prolactin Pro-Differentiation Pathway in Triple Negative Breast Cancer: Impact on Prognosis and Potential Therapy.* Sci Rep, 2016. **6**: p. 30934.
29. Hachim, I.Y., et al., *Prolactin hormone exerts anti-tumorigenic effects in HER-2 overexpressing breast cancer cells through regulation of stemness.* Stem Cell Res, 2019. **40**: p. 101538.
30. Agarwal, N., et al., *Phase I Study of the Prolactin Receptor Antagonist LFA102 in Metastatic Breast and Castration-Resistant Prostate Cancer.* Oncologist, 2016. **21**(5): p. 535-6.
31. Huising, M.O., C.P. Kruiswijk, and G. Flik, *Phylogeny and evolution of class-I helical cytokines.* J Endocrinol, 2006. **189**(1): p. 1-25.
32. Teilum, K., et al., *Solution structure of human prolactin.* J Mol Biol, 2005. **351**(4): p. 810-23.
33. Biener-Ramanujan, E., et al., *Spatio-temporal kinetics of growth hormone receptor signaling in single cells using FRET microscopy.* Growth Hormone & Igf Research, 2006. **16**(4): p. 247-257.
34. Brooks, A.J., et al., *Mechanism of activation of protein kinase JAK2 by the growth hormone receptor.* Science, 2014. **344**(6185): p. 1249783.
35. Liu, Y., et al., *Dynamic analysis of GH receptor conformational changes by split luciferase complementation.* Mol Endocrinol, 2014. **28**(11): p. 1807-19.
36. Cunningham, B.C., et al., *Zinc mediation of the binding of human growth hormone to the human prolactin receptor.* Science, 1990. **250**(4988): p. 1709-12.
37. Kossiakoff, A.A., et al., *Comparison of the intermediate complexes of human growth hormone bound to the human growth hormone and prolactin receptors.* Protein Sci, 1994. **3**(10): p. 1697-705.
38. Fu, Y.K., et al., *Growth hormone augments superoxide anion secretion of human neutrophils by binding to the prolactin receptor.* J Clin Invest, 1992. **89**(2): p. 451-7.
39. Somers, W., et al., *The X-ray structure of a growth hormone-prolactin receptor complex.* Nature, 1994. **372**(6505): p. 478-81.
40. Hughes, J.P. and H.G. Friesen, *The nature and regulation of the receptors for pituitary growth hormone.* Annu Rev Physiol, 1985. **47**: p. 469-82.
41. Frank, S.J., *Classical and novel GH receptor signaling pathways.* Mol Cell Endocrinol, 2020. **518**: p. 110999.
42. Chhabra, Y., et al., *GHR signalling: Receptor activation and degradation mechanisms.* Mol Cell Endocrinol, 2021. **520**: p. 111075.
43. Herman, A., et al., *Functional heterodimerization of prolactin and growth hormone receptors by ovine placental lactogen.* J Biol Chem, 2000. **275**(9): p. 6295-301.
44. Biener, E., et al., *Ovine placental lactogen-induced heterodimerization of ovine growth hormone and prolactin receptors in living cells is demonstrated by fluorescence resonance energy transfer microscopy and leads to prolonged phosphorylation of signal transducer and activator of transcription (STAT)1 and STAT3.* Endocrinology, 2003. **144**(8): p. 3532-40.

555 45. Xu, J., et al., *Growth hormone signaling in human T47D breast cancer cells: potential role for a*
556 *growth hormone receptor-prolactin receptor complex.* Mol Endocrinol, 2011. **25**(4): p. 597-610.
557 46. Liu, Y., et al., *GHR/PRLR Heteromultimer Is Composed of GHR Homodimers and PRLR Homodimers.*
558 Mol Endocrinol, 2016. **30**(5): p. 504-17.
559 47. Liu, Y., et al., *Subdomain 2, Not the Transmembrane Domain, Determines the Dimerization Partner*
560 *of Growth Hormone Receptor and Prolactin Receptor.* Endocrinology, 2017. **158**(10): p. 3235-3248.
561 48. Huang, B., H. Babcock, and X. Zhuang, *Breaking the diffraction barrier: super-resolution imaging*
562 *of cells.* Cell, 2010. **143**(7): p. 1047-58.
563 49. Bates, M., T.R. Blosser, and X. Zhuang, *Short-range spectroscopic ruler based on a single-molecule*
564 *optical switch.* Phys Rev Lett, 2005. **94**(10): p. 108101.
565 50. Kruger, C.L., et al., *Quantitative single-molecule imaging of TLR4 reveals ligand-specific receptor*
566 *dimerization.* Sci Signal, 2017. **10**(503).
567 51. Krüger, C., et al., *Molecular counting of membrane receptor subunits with single-molecule*
568 *localization microscopy*. SPIE BiOS. Vol. 10071. 2017: SPIE.
569 52. Ripley, B.D., *Tests of `Randomness' for Spatial Point Patterns.* Journal of the Royal Statistical
570 Society. Series B (Methodological), 1979. **41**(3): p. 368-374.
571 53. Ester, M., et al., *A density-based algorithm for discovering clusters in large spatial databases with*
572 *noise*, in *Proceedings of the Second International Conference on Knowledge Discovery and Data*
573 *Mining*. 1996, AAAI Press: Portland, Oregon. p. 226–231.
574 54. Mattheyses, A.L., S.M. Simon, and J.Z. Rappoport, *Imaging with total internal reflection*
575 *fluorescence microscopy for the cell biologist.* J Cell Sci, 2010. **123**(Pt 21): p. 3621-8.
576 55. Kohlhuber, F., et al., *A JAK1/JAK2 chimera can sustain alpha and gamma interferon responses.*
577 Mol Cell Biol, 1997. **17**(2): p. 695-706.
578 56. Loesch, K., et al., *Janus kinase 2 influences growth hormone receptor metalloproteolysis.*
579 Endocrinology, 2006. **147**(6): p. 2839-49.
580 57. Deng, L., et al., *Determinants of growth hormone receptor down-regulation.* Mol Endocrinol, 2007.
581 **21**(7): p. 1537-51.
582 58. Zhang, Y., et al., *Growth hormone (GH) receptor (GHR)-specific inhibition of GH-Induced signaling*
583 *by soluble IGF-1 receptor (sol IGF-1R).* Mol Cell Endocrinol, 2019. **492**: p. 110445.
584 59. Jiang, J., et al., *Growth hormone-dependent tyrosine phosphorylation of a GH receptor-associated*
585 *high molecular WEIGHT protein immunologically related to JAK2.* Biochem Biophys Res Commun,
586 1998. **253**(3): p. 774-9.
587 60. Jiang, J., et al., *A conformationally sensitive GHR [growth hormone (GH) receptor] antibody: impact*
588 *on GH signaling and GHR proteolysis.* Mol Endocrinol, 2004. **18**(12): p. 2981-96.
589 61. Beggs, R.R., W.F. Dean, and A.L. Mattheyses, *dSTORM Imaging and Analysis of Desmosome*
590 *Architecture.* Methods Mol Biol, 2020.
591 62. Beggs, R.R., et al., *Desmosomes undergo dynamic architectural changes during assembly and*
592 *maturation.* Tissue Barriers, 2022. **10**(4): p. 2017225.
593 63. Pageon, S.V., et al., *Clus-DoC: a combined cluster detection and colocalization analysis for single-*
594 *molecule localization microscopy data.* Mol Biol Cell, 2016. **27**(22): p. 3627-3636.
595 64. Frank, S.J., *Receptor dimerization in GH and erythropoietin action--it takes two to tango, but how?*
596 Endocrinology, 2002. **143**(1): p. 2-10.
597 65. Cunningham, B.C., et al., *Dimerization of the extracellular domain of the human growth hormone*
598 *receptor by a single hormone molecule.* Science, 1991. **254**(5033): p. 821-5.
599 66. Gent, J., et al., *Ligand-independent growth hormone receptor dimerization occurs in the*
600 *endoplasmic reticulum and is required for ubiquitin system-dependent endocytosis.* Proc Natl Acad
601 Sci U S A, 2002. **99**(15): p. 9858-63.

602 67. Gadd, S.L. and C.V. Clevenger, *Ligand-independent dimerization of the human prolactin receptor*
603 *isoforms: functional implications.* Mol Endocrinol, 2006. **20**(11): p. 2734-46.
604 68. Wilmes, S., et al., *Mechanism of homodimeric cytokine receptor activation and dysregulation by*
605 *oncogenic mutations.* Science, 2020. **367**(6478): p. 643-652.
606 69. Pezet, A., et al., *The last proline of Box 1 is essential for association with JAK2 and functional*
607 *activation of the prolactin receptor.* Mol Cell Endocrinol, 1997. **129**(2): p. 199-208.
608 70. Kassem, N., et al., *Order and disorder-An integrative structure of the full-length human growth*
609 *hormone receptor.* Sci Adv, 2021. **7**(27).
610 71. Bugge, K., et al., *A combined computational and structural model of the full-length human*
611 *prolactin receptor.* Nat Commun, 2016. **7**: p. 11578.
612 72. Ferrao, R.D., H.J. Wallweber, and P.J. Lupardus, *Receptor-mediated dimerization of JAK2 FERM*
613 *domains is required for JAK2 activation.* Elife, 2018. **7**.

614

615

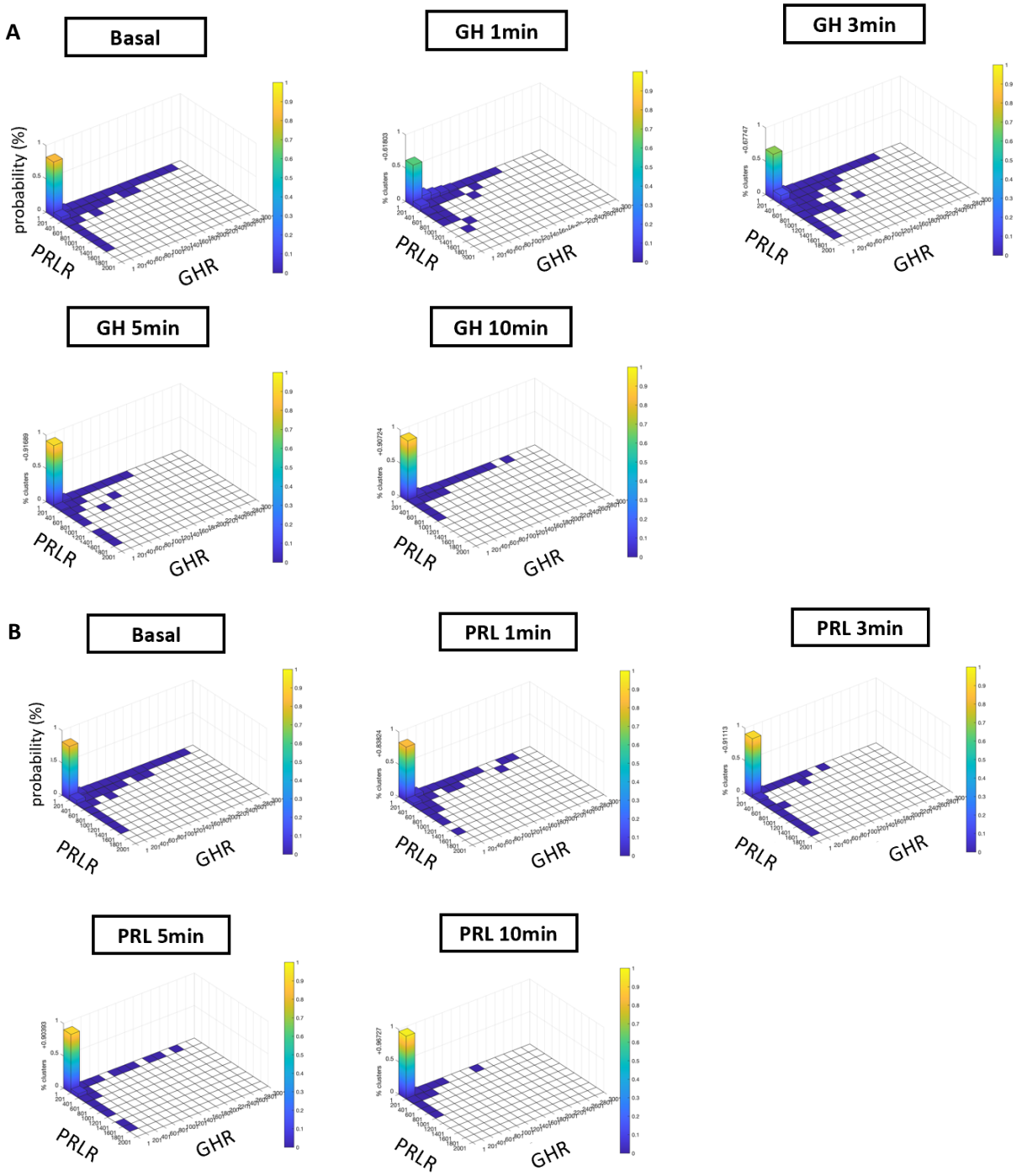

Fig. S1: The size distributions of co-localized clusters are shown in 3D plots, where the binned x-axis represents the number of hGHR localizations, the binned y-axis represents the number of hPRLR localizations, and the z-axis represents the probability of the cluster. Each bin has a size of 200 localizations. Both GH **(A)** and PRL **(B)** induce a distinct change in the composition of co-localized clusters.